Journal of Alloys and Compounds 509 (2011) 6599–6602

Contents lists available at ScienceDirect

Journal of Alloys and Compounds

journal homepage: www.elsevier.com/locate/jallcom

Optical properties of sputtered hexagonal CdZnO films with band gap energies from 1.8 to 3.3 eV

Xiangyang Ma, Peiliang Chen, Ruijie Zhang, Deren Yang*

State Key Laboratory of Silicon Materials and Department of Materials Science and Engineering, Zhejiang University, Hangzhou 310027, China

ARTICLE INFO

Article history:
Received 25 September 2010
Received in revised form 15 March 2011
Accepted 17 March 2011
Available online 29 March 2011

PACS:
78.55.Et
61.66.Dk
81.40.Tv

Keywords:
CdZnO film
Sputtering
Optical properties

ABSTRACT

$Cd_xZn_{1-x}O$ films in a wide range of Cd contents have been grown by reactive direct-current magnetron sputtering. At $x \leq 0.66$, the sputtered $Cd_xZn_{1-x}O$ films are of single hexagonal phase. The optical band gap energies of the $Cd_xZn_{1-x}O$ films decrease from ~3.3 eV at $x = 0$ to ~1.8 eV at $x = 0.66$. Correspondingly, the near-band-edge photoluminescence is tuned in a wide visible region from ~378 to 678 nm. Moreover, the ultraviolet irradiation enhanced PL from the $Cd_xZn_{1-x}O$ films has been observed.

1. Introduction

Owing to the wide band gap (~3.37 eV) at room temperature and large exciton binding energy (~60 meV), ZnO has been considered as a promising candidate for short wavelength optoelectronic applications such as light-emitting diodes or laser diodes [1,2]. It is well known that an important requirement that should be satisfied to develop ZnO-based optoelectronic devices is the modulation of band gap through alloying [3]. Among the materials to narrow the band gap of ZnO, the ternary semiconductor $Cd_xZn_{1-x}O$, alloying ZnO with CdO, is most promising [4,5]. The main reasons are as follows: (1) Cd and Zn ions have similar ionic radii of ~0.74 and 0.60 Å, respectively; (2) CdO has a direct band gap of ~2.3 eV at room temperature, ~1.0 eV narrower than that of ZnO [6,7]. In recent years, a variety of methods have been employed to deposit $Cd_xZn_{1-x}O$ films, such as pulsed laser deposition [4,8], molecular beam epitaxy [9–11], metalorganic vapor-phase epitaxy [12,13], and magnetron sputtering [14]. Unfortunately, ZnO and CdO have different crystal structures as hexagonal and cubic, respectively. Moreover, the thermodynamic solubility of CdO in CdO–ZnO alloying system is quite small i.e. ~2 mol% in thermal equilibrium condition [7,15,16]. Therefore, it is very difficult to grow single-phase hexagonal $Cd_xZn_{1-x}O$ films with high Cd contents. Ishihara et al. employed remote-plasma-enhanced metalorganic chemical vapor deposition to achieve the hexagonal $Cd_xZn_{1-x}O$ films with Cd content as high as $x = 0.69$ [16–18]. However, the method was indeed sophisticated and, moreover, the plasma radical was indispensable for the control of Cd content in a wide range. Currently, preparation of single-phase hexagonal $Cd_xZn_{1-x}O$ films with high Cd contents by simple and widely used methods, such as sputtering, is still a challenge. In this work, $Cd_xZn_{1-x}O$ films have been deposited on Si substrates by reactive direct-current (DC) magnetron sputtering. It is proven that single-phase hexagonal $Cd_xZn_{1-x}O$ films in a wide range of Cd contents, $0 \leq x \leq 0.66$, can be achieved by sputtering. The energy band gaps of the corresponding $Cd_xZn_{1-x}O$ films are modulated from ~1.8 to ~3.3 eV. Furthermore, it is found that the photoluminescence (PL) of $Cd_xZn_{1-x}O$ films can be enhanced by ultraviolet irradiation, the reason of which will be tentatively explained.

2. Experimental details

The $Cd_xZn_{1-x}O$ films with a thickness of ~200 nm were deposited onto Si and quartz substrates by reactive DC magnetron sputtering of a 99.99% pure Cd_yZn_{1-y} ($y = 0, 0.1, 0.2, 0.3, 0.4, 0.6, 0.7, 0.8$, and 1.0) targets. During the sputtering, a mixed gas of oxygen and argon with a flow rate ratio of 1:2 was introduced into the chamber and the working pressure was maintained at ~10 Pa. The sputtering power was ~80 W. The substrate temperature was kept at 500 °C for in situ crystallization of $Cd_xZn_{1-x}O$ films.

* Corresponding author. Tel.: +86 571 8795 1667; fax: +86 571 8795 2322.
E-mail address: mseyang@zju.edu.cn (D. Yang).

0925-8388/$ – see front matter © 2011 Elsevier B.V. All rights reserved.
doi:10.1016/j.jallcom.2011.03.101

The x values of $Cd_xZn_{1-x}O$ films were determined by inductively coupled plasma atomic emission spectrometry (ICP-AES, IRIS Intrepid II XSP, Thermo Electron Corporation). The crystal structures of $Cd_xZn_{1-x}O$ films were characterized by X-ray diffraction (XRD) performed on a Japan Rigaku D/max-ga X-ray diffractometer with graphite monochromatized Cu Kα radiation (λ = 1.54178 Å). The transmission spectra were measured at room temperature using a CARY 100Bio Ultraviolet-Visible Spectrophotometer. The PL spectra were recorded at room temperature using an Acton SpectraPro 2500i Spectrometer and a He–Cd laser (λ = 325 nm) as the excitation source.

3. Results and discussion

Table 1 shows the Cd contents in the sputtered $Cd_xZn_{1-x}O$ films (values of x), determined by ICP-AES, and in the corresponding Cd_yZn_{1-y} targets (values of y). It can be seen that the Cd contents in the films are lower than those in the targets except in the case of $y = 0.1$. Moreover, the Cd content in the film increases with that in the target.

Table 1
Cd contents in sputtered $Cd_xZn_{1-x}O$ films x and in corresponding Cd_yZn_{1-y} alloy targets y.

Cd content in targets, y	0	0.10	0.20	0.30	0.40	0.60	0.70	0.80	1.0
Cd content in films, x	0	0.10	0.14	0.20	0.27	0.52	0.66	0.78	1.0

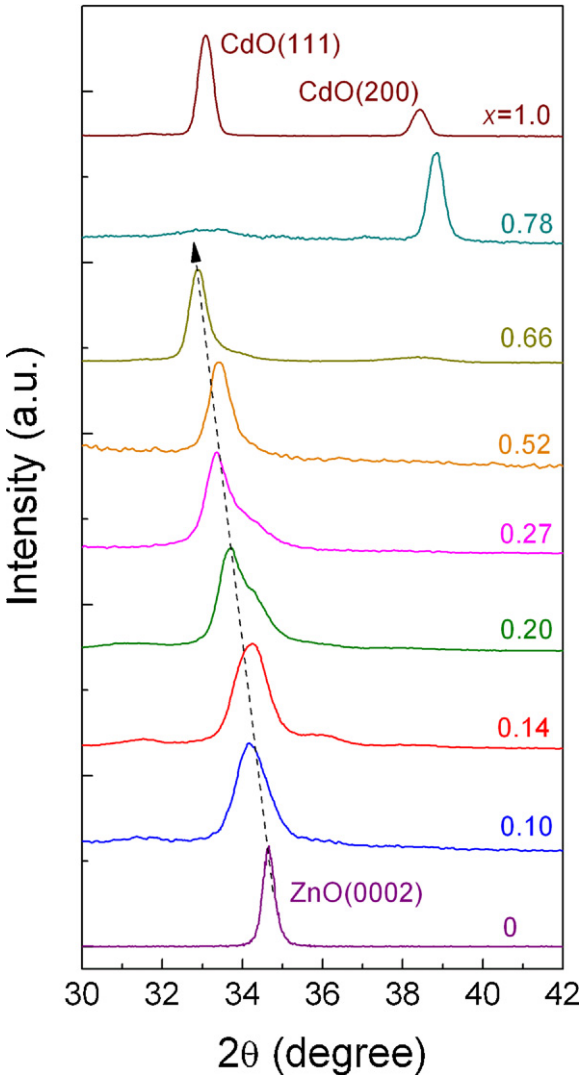

Fig. 1. XRD patterns of the sputtered $Cd_xZn_{1-x}O$ films with different Cd contents x.

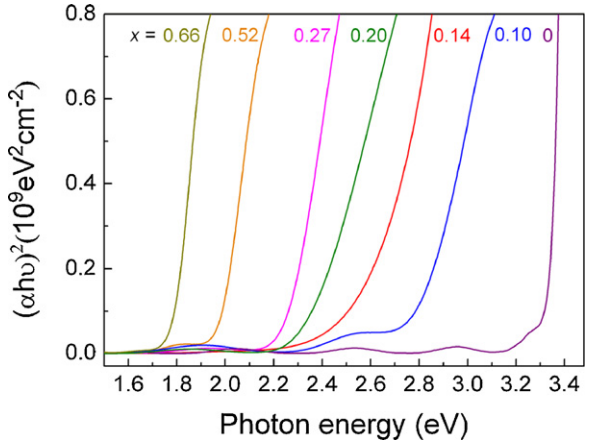

Fig. 2. $(\alpha h\nu)^2$ plots as a function of photon energy $(h\nu)$ for the sputtered $Cd_xZn_{1-x}O$ films.

Fig. 1 shows the XRD patterns of the sputtered $Cd_xZn_{1-x}O$ films on Si substrates with different Cd contents. At $x \leq 0.66$, there is a pronounced peak indexed as the hexagonal (0 0 0 2) in each XRD pattern, indicating that the sputtered $Cd_xZn_{1-x}O$ films are of single hexagonal phase and highly c-axis oriented. It is the non-equilibrium nature of the magnetron sputtering that enables the alloying of CdO and ZnO, as mentioned above. However, the thermodynamic solubility of CdO in CdO–ZnO system is considerably small. In this context, the composition fluctuations in the sputtered $Cd_xZn_{1-x}O$ films are inevitable to occur. It is noticeable that at $0.20 \leq x \leq 0.66$, the hexagonal (0 0 0 2) peak of each $Cd_xZn_{1-x}O$ film has a weak shoulder, which presumably results from the composition fluctuation in the alloys with relatively high Cd contents. Such a shoulder peak, shifted to a larger 2θ with respect to the primary peak, is believed to correspond to the CdZnO alloy with a relatively smaller Cd content. Moreover, the hexagonal (0 0 0 2) peak shifts from ~34.66 to ~32.88° with the increase of x from 0 to 0.66, indicative of the increase of c-axis length of $Cd_xZn_{1-x}O$ with the Cd content. As x increases to 0.78, an obvious peak at ~38.86°, indexed as the cubic (2 0 0) CdO alloyed with ZnO, appears in the XRD pattern. This peak is shifted to a larger 2θ with respect to that of pure CdO because the ion radius of Zn is smaller than that of Cd. Besides, there is a slight peak corresponding to CdO(1 1 1) peak. The above-mentioned result indicates that the cubic CdZnO phase dominates the sputtered film as Cd content is beyond a critical value.

The transmission spectra of the $Cd_xZn_{1-x}O$ films sputtered on quartz substrates were measured, and the absorption coefficients (α) were calculated from the transmittance. Fig. 2 shows $(\alpha h\nu)^2$ plots as a function of photon energy $(h\nu)$ for the $Cd_xZn_{1-x}O$ films, from which the energy band gaps can be calculated. With increasing x, the energy band gap of $Cd_xZn_{1-x}O$ narrows from ~3.3 eV at $x = 0$ to ~1.8 eV at $x = 0.66$. Fig. 3 shows the energy band gaps of the sputtered $Cd_xZn_{1-x}O$ films with different Cd contents. It is well known that the energy band gap of an alloy semiconductor can be conventionally fitted to a bowing formula [6]. In the case of $Cd_xZn_{1-x}O$, the formula can be described as:

$$E_g(x) = (1-x)E_g(\mathrm{ZnO}) + xE_g(\mathrm{CdO}) - bx(1-x)$$
$$= E_g(\mathrm{ZnO}) - (E_g(\mathrm{ZnO}) - E_g(\mathrm{CdO}) + b)x + bx^2 \quad (1)$$

where b is the "optical bowing parameter", $E_g(x)$ is the energy band gap of the $Cd_xZn_{1-x}O$ film at a given Cd content, and $E_g(\mathrm{ZnO})$ and $E_g(\mathrm{CdO})$ are the energy band gaps of ZnO and CdO, respectively. The bowing coefficient b depends on the difference in electronegativities of ZnO and CdO. In this work, the formula for the energy band gap of $Cd_xZn_{1-x}O$ was estimated to be $E_g(x) = 3.3 - 5.3x + 4.7x^2$, which is manifested as the red solid line in Fig. 3.

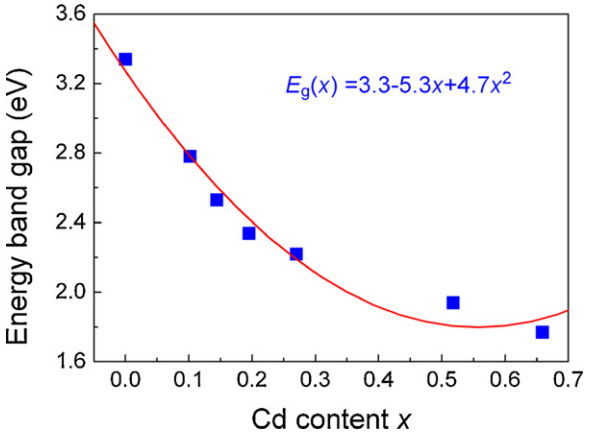

Fig. 3. Energy band gap as a function of Cd content x for the sputtered $Cd_xZn_{1-x}O$ films. Blue squares represent experimental data and red solid line represents the polynomial fitting of the experimental data by using $E_g(x) = 3.3 - 5.3x + 4.7x^2$. (For interpretation of the references to color in this figure legend, the reader is referred to the web version of this article.)

Fig. 4 shows the PL spectra of the $Cd_xZn_{1-x}O$ films with different Cd contents. The PL spectra have been normalized for clarity. It should be mentioned that prior to the PL measurement, some of the $Cd_xZn_{1-x}O$ films were subjected to rapid thermal annealing to enhance the PL while maintaining the hexagonal phase. As can be seen, with increasing x, the near-band-edge (NBE) emission from the $Cd_xZn_{1-x}O$ films is red-shifted from ~378 nm (3.3 eV) at $x = 0$ to ~678 nm (1.8 eV) at $x = 0.66$, showing that the emission from the $Cd_xZn_{1-x}O$ is essentially tunable in a wide visible region.

Furthermore, we observed a phenomenon of ultraviolet (UV)-irradiation enhanced PL of the sputtered $Cd_xZn_{1-x}O$ films. The films were continuously irradiated by a He–Cd laser ($\lambda = 325$ nm), and the PL spectra were recorded at different time intervals. For a typical example, Fig. 5 shows the evolution of PL of the $Cd_{0.66}Zn_{0.34}O$ film with the UV irradiation time. As can be seen, the NBE emission from the $Cd_{0.66}Zn_{0.34}O$ film becomes progressively stronger with the increase of irradiation time. The dependence of spectrally integrated intensity of the NBE emission from the $Cd_{0.66}Zn_{0.34}O$ film on the UV irradiation time is shown in the inset of Fig. 5. Obviously, the UV intensity first increases notably and then keeps nearly constant under further irradiation. Similar features, with the exception of their absolute intensities and NBE emission peaks, were observed in other $Cd_xZn_{1-x}O$ films. The UV-irradiation enhanced PL from the

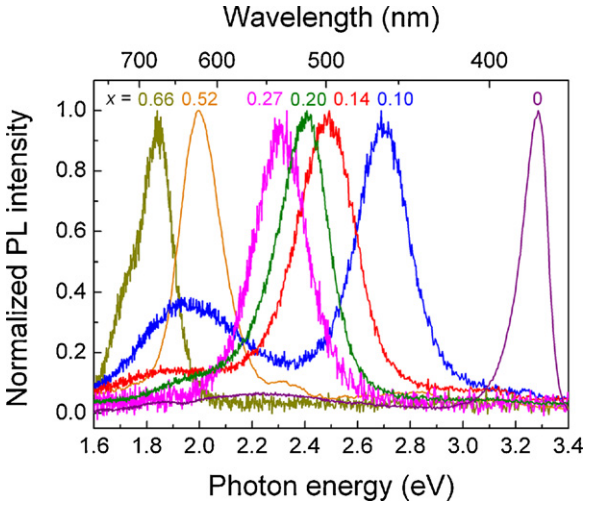

Fig. 4. PL spectra of the sputtered $Cd_xZn_{1-x}O$ films with different Cd contents.

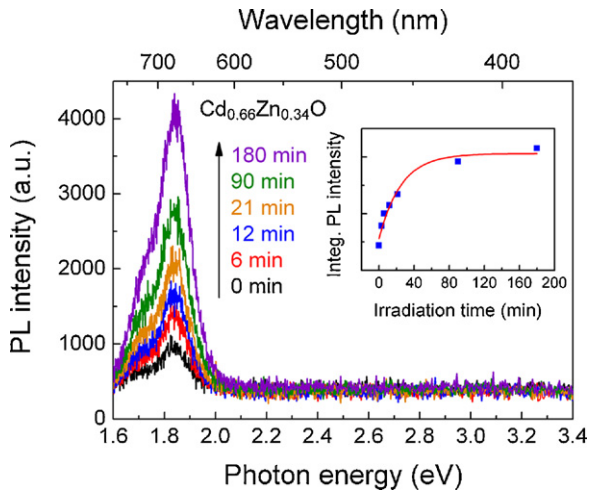

Fig. 5. PL spectra of the $Cd_{0.66}Zn_{0.34}O$ film at different UV irradiation times. The inset shows the dependence of spectrally integrated intensity of the NBE emission of the $Cd_{0.66}Zn_{0.34}O$ film on the UV irradiation time. Blue squares represent experimental data and red solid line represents the exponential fitting of the experimental data. (For interpretation of the references to color in this figure legend, the reader is referred to the web version of this article.)

ZnO films grown by pulsed laser deposition has been previously reported [19]. It is believed that such PL enhancement effect results from oxygen desorption on the surface of ZnO films, which diminishes the amount of negative surface charges thus narrowing the depletion region near the surface. Herein, the $Cd_xZn_{1-x}O$ films were sputtered in a mixed gas of oxygen and argon. Therefore, an amount of oxygen atoms can be adsorbed on the surface of the films, which creates negative surface charges, thus leading to the formation of a wide depletion region near the surface. Owing to the existence of build-in electrical field in the depletion region, the concentration of exciton is decreased. Therefore, the PL in the depletion region is weaker than that in the inside of the films. As the films are subject to the UV irradiation, the photoexcited holes are attracted to the traps such as the oxygen ions at the surface. Due to the hole–trap interaction, the oxygen ions on the film surface substantially disappear. Consequently, the surface depletion region is narrowed, resulting in the enhancement of PL from the $Cd_xZn_{1-x}O$ films.

4. Conclusions

In conclusion, the $Cd_xZn_{1-x}O$ films with a wide range of Cd contents have been grown on Si by reactive DC magnetron sputtering. With x increasing from 0 to 0.66, the c-axis length of hexagonal $Cd_xZn_{1-x}O$ increases, resulting in the shift of diffraction angle of the (0 0 0 2) peaks from ~34.66 to ~32.88°. Moreover, the energy band gap of $Cd_xZn_{1-x}O$ decreases from ~3.3 to ~1.8 eV. Correspondingly, the NBE emissions from the $Cd_xZn_{1-x}O$ films are red-shifted from ~378 to ~678 nm. Furthermore, it is found that the UV irradiation can enhance the PL from the $Cd_xZn_{1-x}O$ films. The preparation of band-gap tunable $Cd_xZn_{1-x}O$ films in this work is believed to be a base for the future development of wavelength tunable light-emitting devices.

Acknowledgments

The authors would like to thank the financial supports from Natural Science Foundation of China (No. 60906024), China Postdoctoral Science Foundation funded project (No. 20080441223), “973 Program” (No. 2007CB613403), Zhejiang Provincial Natural Science Found (No. R4090055), and the foundation of 2008DFR50250 of MOST.

References

[1] Ü. Özgür, Y.I. Alivov, C. Liu, A. Teke, M.A. Reshchikov, S. Doğan, V. Avrutin, S.-J. Cho, H. Morkoç, J. Appl. Phys. 98 (2005), 041301.
[2] S.J. Pearton, D.P. Norton, K. Ip, Y.W. Heo, T. Steiner, Prog. Mater. Sci. 50 (2005) 293.
[3] S. Kalusniak, S. Sadofev, J. Puls, F. Henneberger, Laser Photonics Rev. 3 (2009) 233.
[4] T. Makino, C.H. Chia, N.T. Tuan, Y. Segawa, M. Kawasaki, A. Ohtomo, K. Tamura, H. Koinuma, Appl. Phys. Lett. 77 (2000) 1632.
[5] T. Makino, Y. Segawa, M. Kawasaki, A. Ohtomo, R. Shiroki, K. Tamura, T. Yasuda, H. Koinuma, Appl. Phys. Lett. 78 (2001) 1237.
[6] J.A. Van Vechten, T.K. Bergstresser, Phys. Rev. B 1 (1970) 3351.
[7] A.V. Thompson, C. Boutwell, J.W. Mares, W.V. Schoenfeld, A. Osinsky, B. Hertog, J.Q. Xie, S.J. Pearton, D.P. Norton, Appl. Phys. Lett. 91 (2007) 201921.
[8] H.S. Kang, J.W. Kim, J.H. Kim, S.Y. Lee, Y. Li, J.S. Lee, J.K. Lee, M.A. Nastasi, S.A. Crooker, Q.X. Jia, J. Appl. Phys. 99 (2006), 066113.
[9] X.J. Wang, I.A. Buyanova, W.M. Chen, M. Izadifard, S. Rawal, D.P. Norton, S.J. Pearton, A. Osinsky, J.W. Dong, A. Dabiran, Appl. Phys. Lett. 89 (2006) 151909.
[10] S. Sadofev, S. Blumstengel, J. Cui, J. Puls, S. Rogaschewski, P. Schafer, F. Henneberger, Appl. Phys. Lett. 89 (2006) 201907.
[11] I.A. Buyanova, X.J. Wang, G. Pozina, W.M. Chen, W. Lim, D.P. Norton, S.J. Pearton, A. Osinsky, J.W. Dong, B. Hertog, Appl. Phys. Lett. 92 (2008) 261912.
[12] T. Gruber, C. Kirchner, R. Kling, F. Reuss, A. Waag, F. Bertram, D. Forster, J. Christen, M. Schreck, Appl. Phys. Lett. 83 (2003) 3290.
[13] J. Zuniga-Perez, V. Munoz-Sanjose, M. Lorenz, G. Benndorf, S. Heitsch, D. Spemann, M. Grundmann, J. Appl. Phys. 99 (2006), 023514.
[14] C.W. Sun, P. Xin, C.Y. Ma, Z.W. Liu, Q.Y. Zhang, Y.Q. Wang, Z.J. Yin, S. Huang, T. Chen, Appl. Phys. Lett. 89 (2006) 181923.
[15] H.S. Kang, J.S. Kang, J.W. Kim, S.Y. Lee, J. Appl. Phys. 95 (2004) 1246.
[16] J. Ishihara, A. Nakamura, S. Shigemori, T. Aoki, J. Temmyo, Appl. Phys. Lett. 89 (2006) 091914.
[17] A. Nakamura, J. Ishihara, S. Shigemori, K. Yamamoto, T. Aoki, H. Gotoh, J. Temmyo, Jpn. J. Appl. Phys. 43 (2004) 1452.
[18] S. Shigemori, A. Nakamura, J. Ishihara, T. Aoki, J. Temmyo, Jpn. J. Appl. Phys. 43 (2004) L1088.
[19] C. Jin, A. Tiwari, R.J. Narayan, J. Appl. Phys. 98 (2005) 083707.